Computers and Mathematics with Applications 105 (2022) 107–111

Contents lists available at ScienceDirect

Computers and Mathematics with Applications

www.elsevier.com/locate/camwa

Semi-analytical method for propagation of harmonic waves in nonlinear magneto-thermo-elasticity

C.W. Sahabandu [a,b], M. Dewasurendra [a], Z.A.M.S. Juman [a], K. Vajravelu [c,*], Ali J. Chamkha [d]

[a] Department of Mathematics, University of Peradeniya, Peradeniya 20400, Sri Lanka
[b] Post Graduate Institute of Science, University of Peradeniya, Peradeniya 20400, Sri Lanka
[c] Department of Mathematics, University of Central Florida, Orlando, FL 32816, USA
[d] Faculty of Engineering, Kuwait College of Science and Technology, Doha District, 35004, Kuwait

ARTICLE INFO

Keywords:
Harmonic waves
Magneto-thermo-elasticity
Inverse Mapping
System of partial differential equations

ABSTRACT

In this paper, we develop and apply a semi-analytical method called the Method of Directly Defining inverse Mapping (MDDiM) to obtain a series solution for the propagation of harmonic waves in a nonlinear generalized thermo-elasticity with relaxation time, heating, rotation, and magnetic field. We obtained third-order approximate solutions for the displacement and the temperature fields of the waves with variations in the magnetic field, the relaxation time, and the rotation. The obtained results, with minimum errors, are presented graphically and discussed. Our new extended MDDiM out performs the existing Optimal Homotopy Analysis Method (OHAM) with minimum error and a faster convergent rate. The method can be applied to various systems of nonlinear partial differential equations arising in science and engineering.

1. Introduction

Nonlinear partial differential equations (PDEs) can be used to model many physical systems such as fluid flow, wave propagation, and population dynamics. Finding an analytical solution to a nonlinear partial differential equation is challenging, and techniques for finding solutions exist for only some special cases of nonlinear PDEs. Since many real-world problems can be represented as systems of nonlinear partial differential equations, developing solution techniques for such models are a worthy pursuit. Homotopy Analysis Method (HAM) is one such techniques [1–3]. Liao [1] introduced HAM to solve a nonlinear ordinary differential equation. Later, several investigators [4,5] found out that the HAM does not guarantee a convergent solution. Hence, they introduced the Optimal Homotopy Analysis method (OHAM) to overcome from this obstacle. This Optimal Homotopy Analysis Method is a semi-analytical method used to solve coupled nonlinear ordinary differential equations and systems of nonlinear ordinary differential equations.

Later, Liao [6] introduced an analytical method called the Method of Directly Defining the inverse Mapping (MDDiM). This method significantly reduces the computational time. He used this novel technique to solve a single nonlinear ordinary differential equation. Recently, Dewasurendra et al. [7–10] extended this method to solve systems of coupled nonlinear ordinary differential equations. Later, other researchers (see [11–14]) used successfully this method to solve systems of coupled nonlinear ordinary differential equations arising in real-world applications.

Motivated by the above studies, we extended MDDiM used to solve the systems of nonlinear ordinary differential equations to solve a system of coupled nonlinear partial deferential equations. Further, as an example, we used this new method to analyze the harmonic wave propagation in a nonlinear thermo-elasticity with relaxation time, heating, rotation, and magnetic field [15]. As we know, propagation of harmonic waves appears in the study of circled fuel reactor, high-temperature hydrodynamics, and thermo-elasticity problems. There are several real-world applications that describe this phenomenon such as, magneto-active elastomers which proposed to use in vibration control and robotic applications, thermo-magneto-mechanical coupling framework for magneto-rheological elastomers and continuum modeling approaches [16–18].

2. Methodology

2.1. Construction of the inverse Mapping to solve a system of nonlinear partial differential equations

Consider a system of nonlinear partial differential equations

$$N_j[\bar{u}(\bar{x})] = 0 \quad \bar{x} \in \Omega \quad j = 1, 2, \dots, N, \tag{1}$$

* Corresponding author.
E-mail address: kuppalapalle.vajravelu@ucf.edu (K. Vajravelu).

https://doi.org/10.1016/j.camwa.2021.11.020
Received 11 August 2021; Received in revised form 18 November 2021; Accepted 21 November 2021

subject to the boundary conditions

$$B_{i,j}[\bar{u}(\bar{x})] = \beta_i \quad \bar{x} = \bar{\alpha}_i \quad i = 1, 2, ..., \mu_j, \tag{2}$$

where, $\bar{u}(\bar{x}) = \{u_1(\bar{x}), u_2(\bar{x}), ..., u_N(\bar{x})\}$ is an unknown function, $\bar{x}$ is an independent variable, N_j denotes the non-linear operator, $B_{i,j}$ denotes the linear operator, $1 < \mu_j < n_j$ are positive integers $\bar{\alpha}_i \in \Omega$ and β_i are constants.

By constructing a family of equations with one parameter together with a homotopy parameter $q \in [0, 1]$ to obtain continuous deformation equations,

$$\phi(\bar{x}; q) = \{\phi_1(\bar{x}; q), \phi_2(\bar{x}; q), ..., \phi_N(\bar{x}; q)\},$$

$$(1-q)L_j[\phi_j(\bar{x}; q); u_{0,j}(\bar{x})] = qh_j N_j[\phi(\bar{x}; q)], \quad q \in [0, 1], \tag{3}$$

subject to the conditions

$$(1-q)B_{i,j}[\phi_j(\bar{x}; q); u_{0,j}(\bar{x})] = qh_j B_{i,j}(\phi(\bar{x}; q)) - \beta_{i,j}, \quad \bar{x} = \bar{\alpha}_i. \tag{4}$$

By assuming

$$\phi_j(\bar{x}; q) = u_{0,j}(\bar{x}) + \sum_{k=1}^{+\infty} u_{k,j}(\bar{x}) q^k, \quad \frac{1}{n!} \frac{\partial^k}{\partial q^k} \phi_j(\bar{x}; q)|_{q=0} = D_k \phi_j(\bar{x}; q), \tag{5}$$

and applying homotopy derivative into the zeroth-order equations (3)-(4), one can develop the higher-order deformation equations in the framework of OHAM (see [6] and [7] for more details). However, finding the inverse operator to solve linear sub-problems is still computationally expensive. Here, the freedom of choosing the linear operator in OHAM led Liao to define an inverse linear mapping directly in MDDiM.

Let $S_{\infty,j} = \{\gamma_{1,j}(\bar{x}), \gamma_{1,j}(\bar{x}), ...\}$ be a linearly independent set of infinite number of base functions and define the space function as their linear combination to be $V_j = \sum_{k=0}^{+\infty} \gamma_{k,j}(\bar{x})$. This is, the space where the approximation solution comes from. Next, define the space for the initial guess $V_j^* = \sum_{k=0}^{\mu_j} \gamma_{k,j}(\bar{x})$ by taking a linear combination of the first μ_j functions of the set $S_{\infty,j}$ and $\hat{V}_j = \sum_{k=\mu_j+1}^{+\infty} \gamma_{k,j}(\bar{x})$ so that $V_j = \hat{V}_j \cup V_j^*$. Similarly, let $S_{R,j} = \{\psi_{1,j}(\bar{x}), \psi_{1,j}(\bar{x}), ...\}$ and then define $U_j = \sum_{k=0}^{+\infty} \psi_{k,j}(\bar{x})$ so that $u_j(\bar{x}) \in U_j$. Finally by directly defining the inverse mapping $\mathscr{J} : U_j \longrightarrow V_j$, we obtain the following higher-order deformation equations for the MDDiM.

$$u_{k,j}(\bar{x}) = \chi_k u_{k-1}(\bar{x}) + c_{0,j} \mathscr{J}[\delta_{k-1,j}(\bar{x})] + \sum_{n=1}^{\mu} a_{k,n,j} \varphi_{n,j}(\bar{x}). \tag{6}$$

For the error analysis, we first consider the n-term solution (also called the approximate series solution) $\hat{u}_j(\bar{x}) = u_{0,j}(\bar{x}) + \sum_{k=1}^{n-1} u_{k,j}(\bar{x})$ by using equation (6) and choosing appropriate initial guess $u_{0,j}(\bar{x})$. Then by adding the first n terms of the series solution, we define square residual error functions $E_j(h)$ to find the h values which give the optimal errors, as

$$E_j(h) = \int_{\Omega} (N_j[\hat{u}_j(\bar{x})])^2 d\bar{x} \quad j = 1, 2, ..., N. \tag{7}$$

Sometimes, integration over an infinite domain is difficult. So, we used weighted sum in (8) to calculate the square residual error. Here M is the number of points we wish to use. This Square residual error function is a polynomial in h that can be minimized.

$$E(h) = \frac{1}{M} \sum_{j=0}^{M-1} (\mathcal{N}[\hat{u}])^2 (x_j) \tag{8}$$

2.2. Example: propagation of harmonic waves in non-linear generalized magneto-thermoelasticity under the influence of rotations

Propagation of harmonic waves is very common in thermoelasticity problems, high-temperature hydrodynamics, and study of circled fuel reactor [19,20].

The governing equations of harmonic wave propagation is a system of coupled nonlinear partial differential equations given by (for details see [15])

$$\left(1+\sigma_1\right) u_{tt} + \Omega u_t - u_{xx}\left(1 - \sigma_2 + 2\gamma u_x + 3\delta u_x^2\right) - \beta_1\left(1 - i\omega\tau_2\right)\theta_x - \beta_2\left(\theta u_x\right)_x = 0, \tag{9}$$

$$\left(\theta\left(1 - i\omega\tau_1\right) - a u_x\left(1 - i\omega\delta\tau_1\right) - \frac{1}{2} b u_x^2\right)_t - \left[\left(1 + \alpha u_x\right)\theta_x\right]_x = 0, \tag{10}$$

where, x and t are independent variables, $u(x,t)$ and $\theta(x,t)$ are displacement and the temperature fields respectively, σ_1, σ_2, Ω, γ, β_1, β_2, a, b, and α are arbitrary constants.

The initial conditions are

$$u(x, 0) = \theta(x, 0) = A(1 - \cos(x)), \tag{11}$$

$$u_t(x, 0) = \theta_t(x, 0) = 0. \tag{12}$$

Here, A is an arbitrary constant and the boundary conditions are,

$$u(0, t) = \theta(0, t) = 0, \tag{13}$$

$$u_t(0, t) = \theta_t(0, t) = 0. \tag{14}$$

By taking the left hand side of equations (9) and (10) as the nonlinear equations for this problem, we can write $N_1[u(x,t), \theta(x,t)] = 0$ and $N_2[u(x,t), \theta(x,t)] = 0$ respectively. Now, we defined the sets

$$V = \left\{ \sum_{n=0}^{\infty} c_n (1 - \cos x) t^n \quad | \quad c_n \in R \right\}, \tag{15}$$

$$V^* = \left\{ c_n (1 - \cos x) \quad | \quad c_n \in R \right\} \tag{16}$$

$$\hat{V} = \left\{ \sum_{n=1}^{\infty} c_n (1 - \cos x) t^n \quad | \quad c_n \in R \right\} \text{ and} \tag{17}$$

$$S = \left\{ \sum_{n=0}^{\infty} d_n (1 - \cos x) t^n \quad | \quad d_n \in R \right\}, \tag{18}$$

$$S^* = \left\{ d_n (1 - \cos x) \quad | \quad d_n \in R \right\}, \tag{19}$$

$$\hat{S} = \left\{ \sum_{n=1}^{\infty} d_n (1 - \cos x) t^n \quad | \quad d_n \in R \right\}. \tag{20}$$

Note that $V = V^* \cup \hat{V}$ and $S = S^* \cup \hat{S}$. Let the third-order approximate solutions for $u(x,t)$ and $\theta(x,t)$ be $\sum_{n=0}^{3} u_n(x,t) q^n$ and $\sum_{n=0}^{3} \theta_n(x,t) q^n$ respectively. Plugging $t = 0$ here and comparing coefficients of q^0 together with initial conditions, we obtained initial guesses as

$$u_0(x, t) = A(1 - \cos x) \quad \in V,$$

$$\theta_0(x, t) = A(1 - \cos x) \quad \in S.$$

In the frame of the MDDiM, we have grate privilege to directly defined the inverse mapping, $\mathscr{J} : U_j \longrightarrow \Theta_j$,

$$\mathscr{J}[t^k] = \frac{t^{k+1}}{Bk + 1} \quad \text{for } k \geq 0, \tag{21}$$

where B is constant to be chosen. The special solutions are

$$u_k(x, t) = \chi_k u(x, t)_{k-1} + h\mathscr{J}[D_{k-1}^1] + a_{k,0} + a_{k,1} t \quad \text{for } k \geq 1, \tag{22}$$

$$\theta_k(x, t) = \chi_k \theta(x, t)_{k-1} + h\mathscr{J}[D_{k-1}^2] + b_{k,0} + b_{k,1} t \quad \text{for } k \geq 1, \tag{23}$$

where $a_{k,0}$, $b_{k,0}$, $a_{k,1}$ and $b_{k,1}$ determined by $u_k(x, 0) = 0$, $\theta_k(x, 0) = 0$, $u_k(0, t) = 0$ and $\theta_k(0, t) = 0$ respectively.

Here χ_k is a step function defined by,

$$\chi_k = \begin{cases} 0 & k \leq 1 \\ 1 & k > 1, \end{cases}$$

and

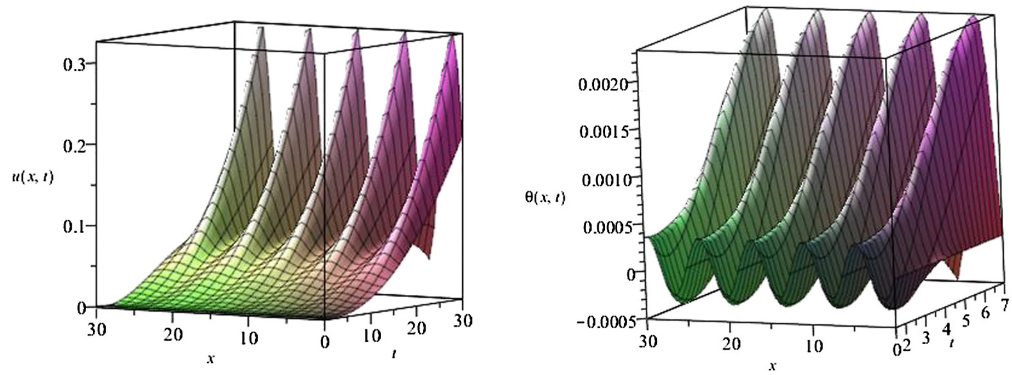

Fig. 1. Solution curves for $u(x,t)$ and $\theta(x,t)$ respectively, when $\tau_1 = 0$ and $\tau_2 = 1$.

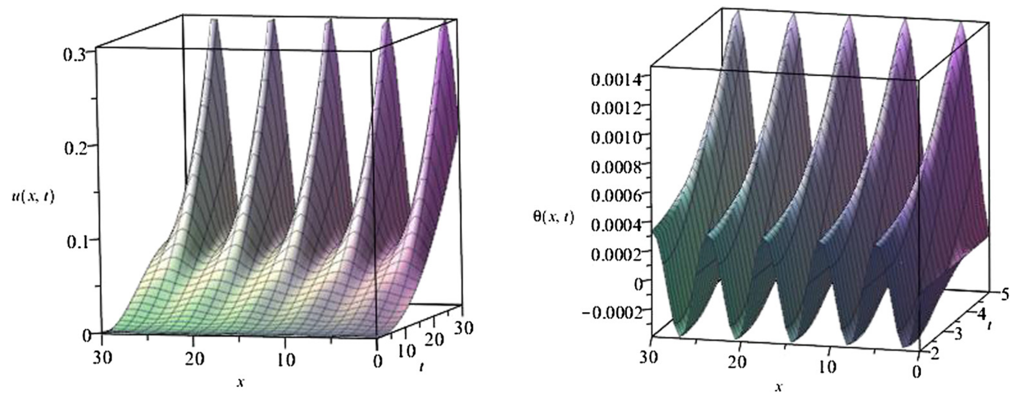

Fig. 2. Solution curves for $u(x,t)$ and $\theta(x,t)$ respectively, when $\tau_1 = 1$ and $\tau_2 = 0$.

$$D^1_{k-1} = \frac{1}{(k-1)!}\left(\frac{\partial^{k-1}}{\partial q^{k-1}} N_1\left[\sum_{n=0}^{3} u_n(x,t)q^n, \sum_{n=0}^{3}\theta_n(x,t)q^n\right]\right), \tag{24}$$

$$D^2_{k-1} = \frac{1}{(k-1)!}\left(\frac{\partial^{k-1}}{\partial q^{k-1}} N_2\left[\sum_{n=0}^{3} u_n(x,t)q^n, \sum_{n=0}^{3}\theta_n(x,t)q^n\right]\right). \tag{25}$$

3. Results and discussion

Using the above equations we obtained the following first four terms of the series solutions for $u(x,t)$ and $\theta(x,t)$ (Figs. 1 and 2).

$$\begin{aligned}
u(x,t) = {} & A(1-\cos x) - 2ht(A\cos x)(1-\sigma_2+3\delta A^2\sin^2 x) + \beta_1 A\sin x) \\
& + 2htA(1-\sigma_2) + h(-(135(A^4\cos x^5\delta^2 + (4/15)A^3\cos x^4\beta_2\delta \\
& - (8/5)\delta((1/3)A\sin x\gamma + A^2\delta + (1/8)A\beta_2 - (1/6)\sigma_2 \\
& + 1/6)A^2\cos x^3 - (11/45((2/11(\alpha\beta_2+(3/2)\beta_1\delta))A\sin x + A^2\beta_2\delta \\
& + (-(2/33)\sigma_2 + 4/33)\beta_2 + (4/33)\beta_1(-\alpha i\omega\tau_2 + \alpha + \gamma)))A\cos x^2 \\
& + ((16/45(A^2\gamma\delta - (1/24)\beta_1\beta_2 - (1/12)\gamma(\sigma_2 - 1)))A\sin x \\
& + (3/5)A^4\delta^2 + (7/45)A^3\beta_2\delta - (2/9)\delta(\sigma_2-1)A^2 \\
& - (1/135)\beta_2(\sigma_2-2)A + (1/135)(\sigma_2-1)^2)\cos x + (((2/135)\alpha\beta_2 \\
& + (1/45)\beta_1\delta)A^2 + (1/135)A\beta_1\beta_2 - (1/135)\beta_1(i\omega\tau_2 + \sigma_2 - 2))\sin x \\
& + (1/45)A(A^2\beta_2\delta + (-(1/3)\sigma_2 + 2/3)\beta_2 \\
& + (2/3)\beta_1(-\alpha i\omega\tau_2 + \alpha + \gamma))))hAt^2/(B+1) \\
& - (135(-(1/45)A^2\Omega\cos x^3\delta + (1/45)\Omega(A^2\delta - (1/3)\sigma_2 + 1/3)\cos x \\
& + (1/135)\sin x\Omega\beta_1 + (1/135)\Omega(\sigma_2-1)))hAt) + \ldots
\end{aligned} \tag{26}$$

$$\begin{aligned}
\theta(x,t) = {} & A(1-\cos x)) - 2ht(\alpha A^2\cos x\sin x + (1+\alpha A\sin x)A\cos x) \\
& + 2htA + h((-\alpha A\cos x h(\alpha A^2\sin x^2 - 2\alpha A^2\cos x^2 \\
& + (1+\alpha A\sin x)A\sin x) - \alpha h(A\cos x(1-\sigma_2+3A^2\delta\sin x^2) \\
& + 18A^3\cos x\sin x^2\delta - 6A^3\cos x^3\delta + \beta_1 A\sin x)A\sin x \\
& - (1+\alpha A\sin x)h(7\alpha A^2\cos x\sin x + (1+\alpha A\sin x)A\cos x) \\
& - \alpha h(A\sin x(1-\sigma_2+3A^2\delta\sin x^2) - 6A^3\cos x^2\delta\sin x \\
& - \beta_1 A\cos x)A\cos x)t^2/(B+1) + (-i\omega\tau_1+1)(h(-\alpha A^2\cos x\sin x \\
& - (1+\alpha A\sin x)A\cos x) + hA)t \\
& + a(\delta i\omega\tau_1 - 1)h(A\sin x(1-\sigma_2+3A^2\delta\sin x^2) - 6A^3\cos x^2\delta\sin x \\
& - \beta_1 A\cos x)t - bA\sin x h(A\sin x(1-\sigma_2+3A^2\delta\sin x^2) \\
& - 6A^3\cos x^2\delta\sin x - \beta_1 A\cos x)t) + \ldots
\end{aligned} \tag{27}$$

The optimal values of h for third-order approximate solutions of (26) and (27) obtained by setting $B = 1$ and $\delta = 1, \sigma_1 = 0.2, \sigma_2 = 0.1, \Omega = 0.1, a = 0.5, A = 0.001, b = 0.5, \alpha = 1, \beta_1 = 0.5, \beta_2 = 0.05, \gamma = 1$ and $\omega = 0.02$ for the following cases (see Table 2 and 4).

Solutions are more accurate when $\tau_1 = 0$ and $\tau_2 = 1$ than $\tau_1 = 1$ and $\tau_2 = 0$ case (see Table 1). The results are presented in Tables 2 and 4.

3.1. Error calculation

We calculated the squared residual errors $E(h)$ of $u(x,t)$ and $\theta(x,t)$ for the four term solutions. To compute the h (converge control parameter) values for two cases, we evaluated the error function defined in equation (28) and minimized it over h. Here we used the equation of weighted sum (see equation (8)) to calculate the errors when $N = M = 50$. (See Figs. 3–6.)

$$E(h) = \frac{1}{N\cdot M}\sum_{i=0}^{N-1}\sum_{j=0}^{M-1}\left(\mathcal{N}_k\left[u\left(\frac{i}{M},\frac{j}{M}\right),\theta\left(\frac{i}{M},\frac{j}{M}\right)\right]\right)^2 \text{ for } k = 1,2 \tag{28}$$

Table 1
MDDiM approximate solutions for u and θ for two cases.

x	t	$u(x,t)$		$\theta(x,t)$	
		When $\tau_1=0$ and $\tau_2=1$	When $\tau_1=1$ and $\tau_2=0$	When $\tau_1=0$ and $\tau_2=1$	When $\tau_1=1$ and $\tau_2=0$
0	0	0	0	0	0
5	5	0.0025188	0.0028808	0.00046146	0.0004615
10	10	0.0204884	0.0219394	0.00850872	0.0046576
15	15	0.0507389	0.0542651	0.02977487	0.0085087
20	20	0.1020411	0.1096074	0.03919234	0.0297775
25	25	0.1214099	0.1280485	0.03975977	0.0397598
30	30	0.0546584	0.0497893	0.39192342	0.3919234

Case I: When $\tau_1=0$ and $\tau_2=1$

Table 2
Comparison of MDDiM results with OHAM results when $\tau_1=0$ and $\tau_2=1$ (order 3).

	MDDiM results		OHAM results	
	h	$E(h)$	h	$E(h)$
$u(x,t)$	−0.36306	6.69465×10^{-7}	−0.97543	7.9675×10^{-7}
$\theta(x,t)$	−0.53009	1.08924×10^{-5}	−0.97543	2.1432×10^{-5}

Table 3
Comparison of MDDiM results of second and third order approximate solutions when $\tau_1=0$ and $\tau_2=1$.

	Second-order		Third-order	
	h	$E(h)$	h	$E(h)$
$u(x,t)$	0.91701	8.06243×10^{-6}	−0.36306	6.69465×10^{-7}
$\theta(x,t)$	−0.52501	1.25752×10^{-5}	−0.53009	1.08924×10^{-5}

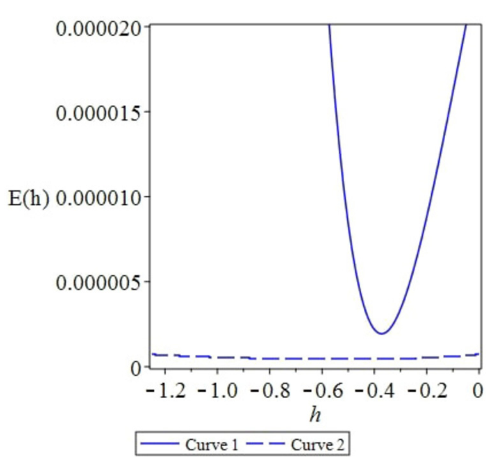

Fig. 3. Corresponding error graphs for $u(x,t)$ and $\theta(x,t)$ are curve 1 and curve 2 respectively, when $\tau_1=0$ and $\tau_2=1$ (order 3).

Case II: When $\tau_1=1$ and $\tau_2=0$

Table 4
Comparison of MDDiM results with OHAM results when $\tau_1=1$ and $\tau_2=0$ (order 3).

	MDDiM results		OHAM results	
	h	$E(h)$	h	$E(h)$
$u(x,t)$	−0.37241	1.93730×10^{-5}	−0.95623	1.37312×10^{-3}
$\theta(x,t)$	−0.53009	4.40052×10^{-7}	−0.95623	1.3242×10^{-2}

Table 5
Comparison of MDDiM results of second and third order approximate solutions when $\tau_1=1$ and $\tau_2=0$.

	Second-order		Third-order	
	h	$E(h)$	h	$E(h)$
$u(x,t)$	0.95968	2.60704×10^{-5}	-0.37241	1.93730×10^{-5}
$\theta(x,t)$	-0.676613	4.60369×10^{-7}	-0.53009	4.40052×10^{-7}

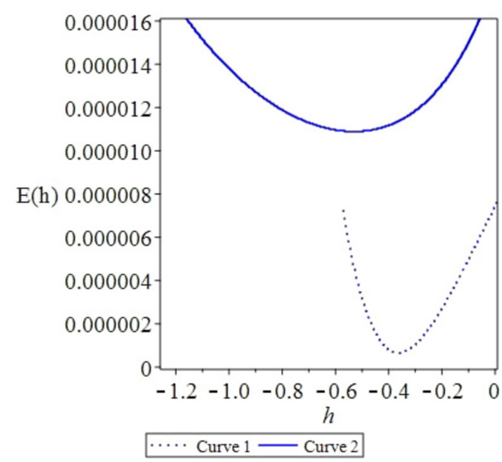

Fig. 4. Corresponding error graphs for $u(x,t)$ and $\theta(x,t)$ are curve 1 and curve 2 respectively, when $\tau_1=1$ and $\tau_2=0$ (order 3).

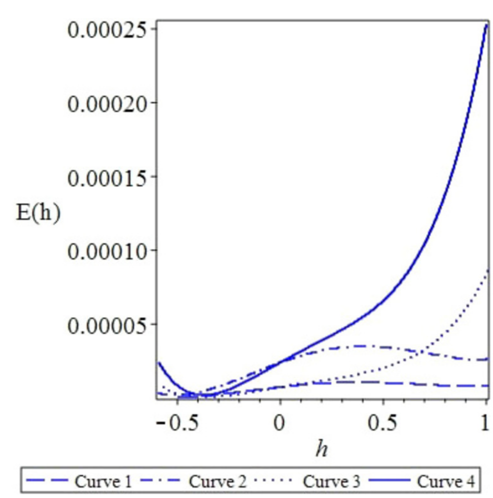

Fig. 5. Corresponding error graphs for $u(x,t)$, for order 2, when $\tau_1=0$ and $\tau_2=1$ curve 1 and when $\tau_1=1$ and $\tau_2=0$ curve 2, and for order 3, when $\tau_1=0$ and $\tau_2=1$ curve 3 and when $\tau_1=1$ and $\tau_2=0$ curve 4, respectively.

When the errors of second and third order approximation solutions of displacement $u(x,t)$ and temperature $\theta(x,t)$ fields are compared, we

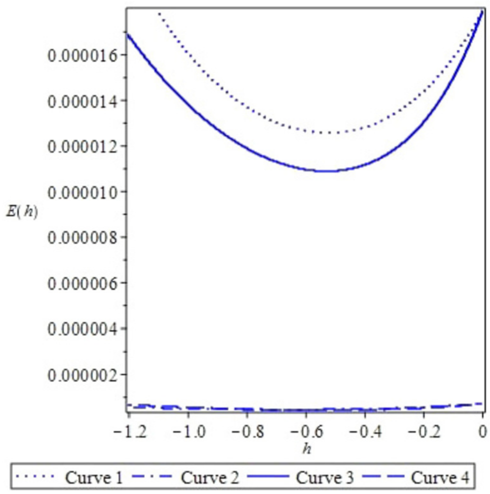

Fig. 6. Corresponding error graphs for $\theta(x,t)$, for order 2, when $\tau_1 = 0$ and $\tau_2 = 1$ curve 1 and when $\tau_1 = 1$ and $\tau_2 = 0$ curve 2, and for order 3 when $\tau_1 = 0$ and $\tau_2 = 1$ curve 3 and when $\tau_1 = 1$ and $\tau_2 = 0$ curve 4, respectively.

can clearly observe that the squared residual errors become smaller when we include higher order terms (see Tables 3 and 5).

In Tables 2 and 3, our MDDiM results are compared with the OHAM results of [15]. From these tables, we can conclude that the convergence rate of MDDiM solutions is much faster than those of OHAM solutions.

4. Conclusions

In this study, we developed the Method of Directly Defining the inverse Mapping to solve a system of coupled nonlinear partial differential equations. The study also shows how to apply MDDiM for a system of coupled partial differential equations and the ability of MDDiM as a relatively efficient computational device for obtaining solutions to problems arising in real-world applications. The computations and graphs associated with the example in this paper are generated using the maple package 16. We obtained the approximate solutions with less complicated terms in terms of series solutions to reduce the computational time. Our MDDiM solutions are in good agreement with the solutions obtained by other analytical methods. By comparing both MDDiM and OHAM results, we can conclude that MDDiM solutions converge much faster than those of the OHAM solutions. Moreover, this novel method can be used to analyze more complicated models that arise in Science and Engineering.

Acknowledgement

The authors thank Dr. A.K. Amarasinghe for editing the manuscript for better English and readability. Also, we would like to express our special thanks to referees for the valuable comments and suggestions to improve the quality of the paper.

References

[1] S. Liao, Proposed Homotopy Analysis Techniques for the Solutions of Nonlinear Problems, Ph.D. thesis, Shanghai Jiao Tong University, 1992.
[2] Y. Tan, S. Abbasbandy, Homotopy analysis method for quadratic Riccati differential equation, Commun. Nonlinear Sci. Numer. Simul. 13 (2008) 539–546.
[3] S.J. Liao, Homotopy Analysis Method in Nonlinear Differential Equations, Springer and Higher Education Press, Heidelberg, 2012.
[4] M. Baxter, R.A. Van Gorder, K. Vajravelu, On the choice of auxiliary linear operator in the optimal homotopy analysis of the Cahn-Hilliard initial value problem, Numer. Algorithms 66 (2014) 269–298.
[5] K. Mallory, R.A. Van Gorder, Optimal homotopy analysis and control of error for solutions to the non-local Whitham equation, Numer. Algorithms 66 (2014) 843–863.
[6] S. Liao, On the method of directly defining inverse mapping for nonlinear differential equations, Numer. Algorithms 72 (2016) 989–1020.
[7] M. Baxter, M. Dewasurendra, K. Vajravelu, A method of directly defining the inverse mapping for solutions of coupled systems of nonlinear differential equations, Numer. Algorithms 77 (2017) 1199–1211.
[8] M. Dewasurendra, M. Baxter, K. Vajravelu, A method of directly defining the inverse mapping for fourth order non-linear systems arising in combined free and forced convection in a second grade fluid, Appl. Math. Comput. 339 (2018) 758–767.
[9] M. Dewasurendra, K. Vajravelu, On the method of inverse mapping for solutions of coupled systems of nonlinear differential equations arising in nanofluid flow, heat and mass transfer, Appl. Math. Nonlinear Sci. 3 (2018) 1–14.
[10] K. Vajravelu, Ronald Li, M. Dewasurendra, Joseph Benarroch, Nicholas Ossi, Ying Zhang, M. Sammarco, K.V. Prasad, Analysis of MHD boundary layer flow of an upper-convected Maxwell fluid with homogeneous-heterogeneous chemical reactions, Commun. Numer. Anal. 2017 (2) (2017) 202–216.
[11] O. Nave, A new method to find the base functions for the method of directly defining the inverse mapping (MDDiM), J. Multiscale Model. 9 (4) (2018) 10.
[12] O. Nave, M. Elbaz, Method of directly defining the inverse mapping applied to prostate cancer immunotherapy—mathematical model, Int. J. Biomath. 11 (5) (2018) 22.
[13] K. Gangadhar, M. Venkata Subba Rao, Sunil Kumar, S. Sharma, S. Munjam, A series-form solution of the coupled nonlinear equations by the method of directly defined inverse mapping and SRM, Int. J. Ambient Energy (2019).
[14] O. Nave, M. Elbaz, Combination of singularly perturbed vector field method and method of directly defining the inverse mapping applied to complex ODE system prostate cancer model, J. Biol. Dyn. (2018).
[15] S.M. Abo-Dahab, M.S. Mohamed, T.A. Nofal, A one step optimal homotopy analysis method for propagation of harmonic waves in nonlinear generalized magnetothermoelasticity with two relaxation times under influence of rotation, Abstr. Appl. Anal. 2013 (2013) 614874.
[16] H. Deng, X. Gong, Application of magnetorheological elastomer to vibration absorber, Commun. Nonlinear Sci. 13 (2008) 1938–1947.
[17] M. Mehnert, M. Hossain, P. Steinmann, Towards a thermo-magneto-mechanical coupling framework for magneto-rheological elastomers, Int. J. Solids Struct. 128 (2017).
[18] M. Mehnert, M. Hossain, P. Steinmann, A complete thermo-electro-viscoelastic characterization of dielectric elastomers, part II: continuum modeling approach, J. Mech. Phys. Solids 157 (2021).
[19] N.H. Sweilam, Harmonic wave generation in non linear thermoelasticity by variational iteration method and Adomian's method, J. Comput. Appl. Math. 207 (1) (2007) 64–72.
[20] A.N. Abd-Alla, A.F. Ghaleb, G.A. Maugin, Harmonic wave generation in nonlinear thermoelasticity, Int. J. Eng. Sci. 32 (7) (1994) 1103–1116.